

Subthreshold antiproton production in proton-carbon reactions

V I Komarov¹, H Müller² and A Sibirtsev³

¹ Joint Institute for Nuclear Research, LNP, 141980 Dubna, Russia

² Institut für Kern- und Hadronenphysik, Forschungszentrum Rossendorf, D-01314 Dresden, Germany

³ Institut für Kernphysik, Forschungszentrum Jülich, D-52425 Jülich, Germany

E-mail: H.Mueller@fz-rossendorf.de

Abstract. Data from KEK on subthreshold \bar{p} as well as on π^\pm and K^\pm production in proton-nucleus reactions are described at projectile energies between 3.5 and 12.0 GeV. We use a model which considers a hadron-nucleus reaction as an incoherent sum over collisions of the projectile with a varying number of target nucleons. It samples complete events and allows thus for the simultaneous consideration of all particle species measured. The overall reproduction of the data is quite satisfactory. It is shown that the contributions from the interaction of the projectile with groups of several target nucleons are decisive for the description of subthreshold production. Since the collective features of subthreshold production become especially significant far below the threshold, the results are extrapolated down to COSY energies. It is concluded that an \bar{p} measurement at ANKE-COSY should be feasible, if the high background of other particles can be efficiently suppressed.

PACS numbers: 24.10.-i, 24.10.Lx, 25.40.-h

1. Introduction

Subthreshold particle production in a nuclear reaction is understood as production below the energy threshold of the considered process in a free nucleon-nucleon (NN) collision. It is thus a nuclear phenomenon which may be explained by rather different assumptions on the properties of nuclear matter and on the interaction dynamics. Hereby it is an open question to what extent subthreshold particle production is governed by properties of the nuclear ground state wavefunction and to what extent by the dynamical properties of nuclear matter, not reflected in the ground state description. The problem is far from a final solution at present and evidently requires a systematic study of high-momentum transfer processes, among them subthreshold particle production.

At COSY a research programme is in progress which is devoted to the systematic investigation of subthreshold particle production. Subthreshold production of K^+ mesons [1] was one of the foundations for the design and building of the ANKE spectrometer [2], which allows for the measurement of K^+ meson production cross sections under the condition of an extremely high background of other particles. Recently, first results [3, 4, 5] on K^+ meson production have been published. Moreover, it was proposed [6] to extend the research programme to the subthreshold production

of K^- mesons. This made a considerable extension of the ANKE spectrometer necessary, because additional equipment for the registration of negative particles had to be installed.

Following this line, in this paper the question is examined if the investigation of subthreshold \bar{p} production is manageable at COSY energies. The highest energy of 2.8 GeV reached at COSY up to now is far below the threshold energy of 5.63 GeV for \bar{p} production in NN interactions. This makes the measurement a real challenge due to the low cross section and due to the high background of other particles. From the physical point of view, however, deep subthreshold production far below the threshold becomes especially interesting, because the collective aspects of the phenomenon can be expected to become more and more dominating. Indeed, the created mass in case of \bar{p} production (1.876 GeV) is essentially higher compared to K^+ production (0.67 GeV), and the energy is 2.83 GeV below the NN threshold if a \bar{p} production experiment would be carried out at 2.8 GeV. Such a difference is significantly larger than the value of 0.58 GeV achieved so far at ANKE in the K^+ production experiments at an energy of 1 GeV [3].

First measurements of subthreshold \bar{p} production in proton-nucleus collisions at higher energies had been carried out [7, 8, 9, 10] a few decades ago. Then investigations in nucleus-nucleus collisions [11, 12, 13, 14, 15] and more recent studies of proton-nucleus reactions [16, 17, 18] followed. Most of the descriptions proposed so far are based on transport calculations [19, 20, 21, 22, 23, 24, 25, 26, 27, 28], thermodynamical considerations [29, 30, 31, 32] or multi-particle interactions [33]. All these approaches consider the \bar{p} spectra without any relation to measurements of the other reaction channels. At KEK [18], however, the spectra of π^\pm and K^\pm mesons were measured together with those of the antiprotons. The present approach is distinguished by considering simultaneously all these reaction channels. This allows for a more comprehensive determination of the model parameters and makes a prediction for COSY more profound.

It should be stressed that the investigation of subthreshold production in connection with the other reaction channels is also of great importance for the understanding of this process. Fragmentation of the target residue is such a distinguished channel having a large cross section. In a participant-spectator picture there seems to be rather a weak connection between the interaction of the participants leading to particle production and the excitation of the residual nucleus during this process. At subthreshold energies, however, the competition between these two energy consuming processes may heavily influence the cross sections observed. In [34] this question was considered for proton-induced subthreshold production of K^+ mesons. There, the interplay of subthreshold production and the fragmentation of the residual nucleus was investigated in the Rossendorf collision (ROC) model, which allows the treatment of hadronic and nuclear reactions in a unified way. Here, we extend these considerations to the case of subthreshold \bar{p} production. Both the fragmentation of the residual nucleus and the interaction of the nucleons participating in the scattering process are treated on the basis of analogous assumptions. Even more important, the phase-space of the complete final state including the reaction products of the projectile-participant interaction as well as the fragments of the decay of the spectator system is exactly calculated. To the best of our knowledge this feature seems to be unique to the ROC model.

In the ROC model the nuclear residue becomes excited during the reaction due to the distortion of the nuclear structure by the separation of the participants

from the spectators and due to the passage of the reaction products through the spectator system. In this global way final-state interactions are taken into account without making special assumptions concerning re-absorption, re-scattering, self-energies, potentials etc. for the various particle types. The discussion of these properties is rather controversial. If one considers *e.g.* re-absorption of \bar{p} then the treatment reaches from no explicit consideration [33, 35] over a global factor 0.1 for $p+Cu$ [20] to taking the mean free path into account [21]. For $Si+Si$ the survival rates of antiprotons are according to [23, 24, 19] in the region of several %, while in [36] a reduction of about 50% for $p+Au$ and $Si+Au$ from an analysis of \bar{p} production at higher energies [37] has been reported. The authors [18] conclude from an analysis of the target-mass dependence of their data that re-absorption of \bar{p} is much smaller than expected from the corresponding $\bar{p}N$ cross section. Thus, it is far from being clear to what degree antiprotons are absorbed in the nuclear medium.

The plan of the paper is as follows. In section 2 the main ingredients of the ROC model are explained, which is used for the calculations to be presented. Section 3 contains a comparison of theoretical and experimental results for particle production and fragmentation with special emphasis on subthreshold \bar{p} production. A prediction of the antiproton cross section at COSY energies and a comparison with the cross sections for π^- and K^- production is made in section 4. A summary is given in section 5.

2. The model

The ROC model is implemented as a Monte Carlo generator which samples complete events for hadronic as well as nuclear reactions. It makes no detailed assumptions on the intra-nuclear development of the interaction process, but calculates instead the statistical weights of the possible final states. The dynamics of the reaction is taken into account in form of empirical functions which modify the population of the final states. This is in contrary to transport models, where the interaction of the projectile with target nucleons and the subsequent interactions of particles originating from primary collisions with further target nucleons are modelled. The ROC approach does not need any parameterisation of elementary cross sections. Its applicability is not restricted at higher energies by the growing number of unknown elementary cross sections. All dynamic information is gathered in a few parameters which are either constant or change smoothly with energy and/or target mass. The energy necessary for subthreshold production stems from interactions of the projectile with few-nucleon groups, also called clusters in the following, and from the Fermi motion of these clusters.

The model was successfully tested for pp interactions up to ISR energies in [38, 39], while nuclear reactions were considered in the papers [34, 40, 41, 42]. In the following the basic ideas of the ROC model relevant for this paper are summarised.

The cross section of the interaction of an incoming hadron with a target nucleus (A, Z) consisting of $A - Z$ neutrons and Z protons is calculated as an incoherent sum over contributions from a varying number a of nucleons (thereof z protons) participating in the interaction

$$d\sigma(s) = \sum_{a=1}^A \sum_{z=\max(0, a-Z)}^{\min(a, Z)} \sigma_{az} \frac{dW(s; \alpha_{az})}{\sum_{\alpha_{az}} dW(s; \alpha_{az})}. \quad (1)$$

Here, $s = P^2$ denotes the square of the centre-of-mass energy of the projectile-target system with $P = (E, \vec{P})$ being the total four-momentum, σ_{az} stands for the partial cross section of the interaction of the projectile with a cluster (a, z) , and the quantities $dW(s; \alpha_{az})$ describe the relative probabilities of the various final channels α_{az} .

The partial cross sections σ_{az} account for sequential collisions between projectile and a nucleons of the target. Such a sequence is treated in the ROC model as a collision between the incident particle and a cluster consisting of a nucleons capable of sharing their energy in close analogy with the virtual clusters of the cooperative model [43, 44, 45, 46, 47, 48, 49, 50]. The σ_{az} are calculated using a modified version of the Monte Carlo code [51] which is based on a probabilistic interpretation of the Glauber theory [52]. We use the profile function

$$\Gamma_A(b) = \int \left[1 - \prod_{i=1}^A (1 - p_i) \right] \prod_{i=1}^A \rho_A(\vec{r}_i) d^3 r_i$$

of the considered nucleus, which depends on the nucleon density $\rho_A(\vec{r}_i)$ and the probability

$$p_i = \exp(-d_i^2 \pi / \sigma_{NN})$$

for an interaction of the projectile and the i th target nucleon with d_i being the distance between the interacting particles. The nucleon density [53]

$$\rho_A(\vec{r}) \propto (1 + \eta[1.5(f^2 - e^2)/f^2 + e^2 r^2/f^4]) \exp(-r^2/f^2) \quad (2)$$

of light nuclei $A < 20$ can be derived from a standard shell model wavefunction with $\eta = (A - 4)/6$, $f^2 = e^2(1 - 1/A)$ and $f = 1.55$ fm. Then the NN cross section σ_{NN} is adapted such that the integral of the profile function over the impact parameter b reproduces the total inelastic pA cross sections

$$\sigma_{pA}^{\text{in}} = \int d^2 b \Gamma_A(b),$$

which are approximately constant in the energy region under consideration. The same calculation yields also the partial cross sections σ_{az} we are interested in (for further details see [51]).

The relative probabilities of the various final channels α_{az} in (1)

$$dW(s; \alpha_{az}) \propto dL_n(s; \alpha_{az}) \rho_A(\vec{P}_R) T^2(\alpha_{az}) \quad (3)$$

are given by the Lorentz-invariant phase-space factor $dL_n(s; \alpha_{az})$ multiplied by the square of the empirical reaction matrix element $T^2(\alpha_{az})$ responsible for the collision dynamics. The Fermi motion is implemented via the momentum distribution of the residual nucleus $\rho_A(\vec{P}_R)$, which is made a function of the number of participants a . It is taken as a Gaussian having a width of

$$\sigma_a = \sqrt{a(A - a)/5/(A - 1)} p_F \quad (4)$$

in accordance with the independent particle model [54] with p_F being the Fermi-limit of the nucleus considered. No special high-momentum component [35, 55, 56, 57, 58, 59] is used in this paper.

The Lorentz-invariant phase-space is defined as the integral over the four-momenta of the n primarily produced final particles with energy-momentum conservation taken into account

$$dL_n(s; \alpha_{az}) = \prod_{i=1}^n d^4 p_i \delta(p_i^2 - m_i^2) \delta^4(P - \sum_{i=1}^n p_i). \quad (5)$$

Here, the four-momentum of the i -th particle is denoted by $p_i = (e_i, \vec{p}_i)$ with $p_i^2 = m_i^2$.

For numerical calculations the δ -function in equation (5) has to be removed by introducing a new set of $3n - 4$ variables to replace the $3n$ three-momentum components. It is reasonable to choose a set of variables, which reflects the underlying physical picture of the interaction process. Using recursion [60] equation (3) can be rewritten in the form (see Appendix)

$$dW(s; \alpha_{az}) \propto \frac{d^3 P_R}{2E_R} \rho_A(\vec{P}_R) dW_R(M_R^2) dW_P(M_P^2). \quad (6)$$

Here, the four-momenta of the nuclear residue $P_R = (E_R, \vec{P}_R)$ and of the participants

$$P_P = P - P_R = (E_P, \vec{P}_P), \quad (7)$$

yield the corresponding invariant masses according to $M_R^2 = P_R^2$ and $M_P^2 = P_P^2$. The integral over the Fermi motion $d^3 P_R \rho_A(\vec{P}_R)/2E_R$ separates the phase-space of the n_R nuclear fragments

$$dW_R(M_R^2) = dM_R^2 dL_{n_R}(M_R^2) T_R^2(\alpha_{az}^R) \quad (8)$$

from the phase-space

$$dW_P(M_P^2) = dL_{n_P}(M_P^2) T_P^2(\alpha_{az}^P) \quad (9)$$

of the $n_P = n - n_R$ final particles arising from the participant system. In (8) and (9) the matrix element

$$T^2(\alpha_{az}) = T_R^2(\alpha_{az}^R) T_P^2(\alpha_{az}^P) \quad (10)$$

is split into two factors describing residue fragmentation into channel α_{az}^R and participant interaction resulting in channel α_{az}^P , accordingly. There is, however, a strong kinematic link between participants and spectators, since invariant mass M_P of the participant system, invariant mass M_R of the residue and the relative kinetic energy $\sqrt{s} - M_P - M_R$ of these two particle groups are connected by energy-momentum conservation. For particle production to proceed the invariant mass of the participants must exceed the corresponding threshold value M_P^{th} which in turn depends on the number of participants. The heavier the effective target is the more energy is available for particle production. Another way to reach the threshold value goes via the Fermi motion, since the participant mass is a function of the momentum vector of the nuclear residue. The excitation energy of the target residue comes usually into play via the spectral function (see *e.g.* [56]) derived from electron scattering data. Unique to the ROC model, however, is the treatment of the spectator system in close analogy with the participant subsystem. The ROC model calculates the complete final state of both the participants and the spectators. Thus, the huge amount of final channels of the spectator fragmentation influences directly the final state of the participant system and vice versa.

The term $dW_P(M_P^2)$ in (6), (9) describes the interaction of the incoming proton with the group of participating target nucleons. Such a projectile-cluster reaction is treated in complete analogy to a hadronic reaction. In a first step intermediate particle groups called fireballs (FBs) are produced, which decay into so-called primary particles. The primary particles define the channels for which the weights (9) are calculated. Among them are resonances, which decay subsequently into stable hadrons. In case of the presence of several nucleons among the decay products of a FB they may form nuclear fragments with equal probability for all possible channels.

The dynamical input of the reaction is implemented by the empirical transition matrix element

$$T_P^2(\alpha_{az}^P) = T_i^2 T_{qs}^2 T_{ex}^2 T_t^2 T_l^2 T_{st}^2, \quad (11)$$

which describes the interaction process T_i^2 resulting in the production of a varying number N of FBs ($N \geq 2$), the production of hadrons T_{qs}^2 via the creation of quark-antiquark ($q\bar{q}$) pairs, the invariant-mass distribution of the FBs T_{ex}^2 , the transverse T_t^2 and longitudinal T_l^2 momentum distribution of the FBs, and, finally, some factors T_{st}^2 necessary for the calculation of the statistical weights. The interaction is assumed to proceed via colour exchange leading to the removal of valence quarks or of gluons from the interacting hadrons. Additional up, down and strange quark pairs are created in the ratio

$$u : d : s = 1 : 1 : \lambda_s \quad (12)$$

with $\lambda_s = 0.15$. They form the varying number of FBs, which subsequently decay into the final hadrons. The transverse momenta of the FBs are restricted by an exponential cut-off (longitudinal phase-space) according to

$$T_t^2 = \prod_{I=1}^N \exp(-\gamma P_{t,I}) \quad (13)$$

with the mean $\bar{P}_t = 2/\gamma$. Two leading FBs, the remnants of the incoming hadron and of the cluster, get in the mean larger longitudinal momenta than the central FBs by weighting the events with

$$T_l^2 = (X_1 X_2)^\beta. \quad (14)$$

Here, the light-cone variables $X_1 = (E_1 + P_{z,1})/(e_b + p_{z,b})$ and $X_2 = (E_2 - P_{z,2})/(E_P - P_{z,P})$ are used with the four-momentum of the projectile given by $p_b = (e_b, \vec{p}_b)$ and that of the participants by (7). Each FB is characterised by two parameters, a temperature Θ_{FB} and a volume V_{FB} . The temperature determines the relative kinetic energy of the particles the FB decays into via

$$T_{ex}^2(\Theta_{FB}) = \prod_{I=1}^N (M_I / \Theta_{FB}) K_1(M_I / \Theta_{FB}), \quad (15)$$

while the volume defines the interaction region and influences mainly the particle multiplicity via the statistical factor $T_{st}^2 \propto V_{FB}^{n_P-1}$. In (15) K_1 stands for the modified Bessel function. Final hadrons are built-up by random recombination of the available quarks during the decay of the FBs. This procedure ensures automatically the conservation of all internal quantum numbers. Resonances decay later on until the final state consisting of stable particles is reached. For a more detailed discussion of the hadronic matrix element the reader is referred to [39]. In this paper we use the same set of parameters as in [39] for the description of the interaction of the projectile with a single target nucleon. Most of the other terms in (1), however, contain clusters consisting of several target nucleons. The basic parameters of the FBs emerging from such an interaction are fixed by scaling the volume with the number of cluster nucleons a and the temperature parameter with $a^{-1/3}$ according to

$$V_{FB} = V_{FB}^0 a \quad \text{and} \quad \Theta_{FB} = \Theta_{FB}^{max} a^{-1/3}. \quad (16)$$

It remains to consider the target residue, the structure of which is strongly disturbed by the projectile-participant reaction and subsequent final-state

interactions. This leads to the excitation and decay of the spectator system, which is characterised by the two parameters temperature Θ_R and volume V_R in the same way as the FBs emerging from the projectile-participant interaction. The part of the matrix element responsible for the residue fragmentation

$$T_R^2(\boldsymbol{\alpha}_{az}^R) = T_{\text{ex}}^2(\Theta_R) T_{\text{st}}^2(\boldsymbol{\alpha}_{az}^R)$$

is identical with the corresponding factors (11) applied to the hadronic FBs. In order to restrict the excitation energy transferred to the residue we use the asymptotic approximation of (15) for large mass M_R and small temperature Θ_R

$$T_{\text{ex}}^2(\Theta_R) = \sqrt{M_R/\Theta_R} \exp(-M_R/\Theta_R). \quad (17)$$

An impact parameter dependence is assumed for the temperature parameter. This seems to be reasonable, because a peripheral collision with only few participating nucleons should excite the nuclear residue much less than a central collision with many participants. As a first guess we use

$$\Theta_R = \Theta_R^{\max} [1 - \exp(-a/\bar{a}A^{1/3})] \quad (18)$$

with \bar{a} as parameter, here fixed to $\bar{a} = 0.5$, which determines how fast the maximal temperature Θ_R^{\max} is reached with increasing number of participants a .

All factors still necessary for a correct calculation of the relative weights of the various channels are collected in complete analogy with the corresponding factors for the FBs in the term

$$T_{\text{st}}^2(\boldsymbol{\alpha}_{az}^R) = g(\boldsymbol{\alpha}_{az}^R) \left(\frac{V_R}{(2\pi)^3} \right)^{n_R-1} \prod_{i=1}^{n_R} (2\sigma_i + 1) 2m_i. \quad (19)$$

It contains the spin degeneracy factors $(2\sigma_i + 1)$, the volume V_R in which the particles are produced with $V_R = 4\pi(A-a)R_R^3/3$ determined by the radius parameter R_R . The quantity $g(\boldsymbol{\alpha}_{az}^R)$ is the degeneracy factor for groups of identical particles in the final state of the residue decay and prevents multiple counting of identical states.

Temperature and volume determine as in the case of hadronic reactions the number of final particles and their relative energy. The main difference consists in the value of the temperature parameter, $\Theta_{FB}^{\max} \approx 300 \text{ MeV}$ for hadronic and $\Theta_R^{\max} \approx 10 \text{ MeV}$ for nuclear systems. New particles can be produced in hadronic reactions, while for nuclear systems, due to the much lower temperature, the nucleons of the initial state are recombined into various fragments without producing new hadrons. The volume parameter defines the distance between the fragments where the strong interaction ceases to work. This volume goes into the calculation of the weight of the final state. Due to the long range of the Coulomb repulsion Coulomb energy is still stored in the system at those distances. This energy is calculated in the Wigner-Seiz-approximation (see [61]). The random distribution of the Coulomb energy among the charged fragments yields the final momenta of the fragments at large distances.

In the calculation we assume that the fragments emerging from the residue decay are stable against particle decay. The possibility of hot fragments cooling down by subsequent particle emission is also implemented in the model (see [34]), but it turned out that a readjustment of the volume and/or the temperature parameter yields quite similar results in both cases. So we decided in favour of the easier approach. Moreover, for a light nucleus as ^{12}C this question is of minor importance.

In concluding this section it should be mentioned, that it is the calculation of the relative probabilities $dW(s; \alpha_{az})$, equation (3), which makes the difference between the cooperative [43, 44, 45, 46, 47, 48, 49, 50] and the ROC model, although the notion of clusters is similar in both approaches. In the cooperative model the relative probabilities of the various channels are calculated in the pure phase-space limit and the excitation and decay of the target residue is completely neglected. In contrast, the ROC model is far from being a pure statistical approach, because it contains specific information on the properties of nuclei and the interaction of the projectile with few-nucleon groups (clusters) in the nucleus. The model includes strong assumptions on the amplitude of the projectile-cluster interaction which lead to the restriction of excitation energy and momentum transfer to clusters compared to pure phase-space. A further nontrivial assumption concerns the various possibilities for the dissipation of the transferred energy inside the hit clusters either as relative kinetic energy of the decay products or as newly produced particles. In extreme cases the whole energy can be completely accumulated for the production of new particles. The other extreme is the emission of very fast secondaries with energies outside the kinematical limits of a projectile-(single)nucleon interaction without producing new particles. Also the supposition that clusters behave themselves like hadrons with respect to quark statistics is of great importance for the relative weights of the various final reaction channels. All these assumptions form a new approach to the consideration of local excitations and may, therefore, give essential and definite information on the properties of nuclear matter (excitation probability, distribution of deposited energy and transferred momenta, decay modes of few-nucleon fireballs etc).

3. Comparison with data

In order to fix the parameters describing the Fermi motion and the decay of the residue we consider the energy spectra of fragments from the reaction of 2.1 GeV protons with carbon measured at 90° (see figure 1). For the volume a radius $R_R = 1.7$ fm is taken. This corresponds to about 1/3 of normal nuclear density and is within the region of break-up densities used for example by [63]. In figure 1 the heaviest fragment, C , arises mainly from the quasi-free interaction of the incoming proton with a single target neutron and may gain energy only from the Fermi motion. Thus, the spectrum is highly sensitive to the width σ_a , equation (4), of the Gaussian for the Fermi motion. On the other hand, the lightest fragments are decay products of the residue and their kinetic energy in the laboratory is a superposition of Fermi motion and relative kinetic energy of the residue fragments. A satisfactory description of the fragment spectra in figure 1 is achieved using $\Theta_R^{max} = 12$ MeV, equation (18), and $p_F = 320$ MeV/c, equation (4). No attempt was made to improve the description of the spectra by implementing an additional high-momentum component, although especially the high-momentum parts of the spectra of the heavier fragments are underestimated. The spectator-participant picture is an idealisation, and not only the nuclear wavefunction but also secondary interactions between spectators and participants might be responsible for the observed deviations. All the following calculations are carried out with the above fixed values for Θ_R^{max} and p_F . It should be stressed in this connection that temperature Θ_R and volume parameter R_R of the nuclear residue are highly correlated, a fact already observed in [39] for the FB parameters in hadronic reactions.

In figure 2 the momentum spectra of π^\pm and K^\pm mesons as well as of \bar{p} are

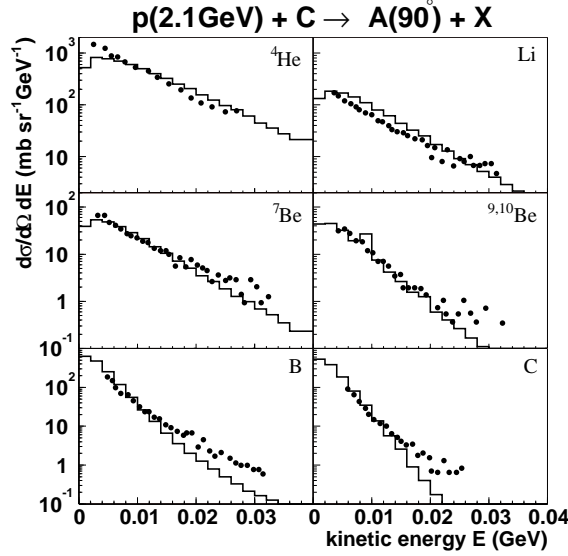


Figure 1. Differential cross section as function of the kinetic energy of fragments produced in the reaction of protons with carbon [62] (dots) compared to ROC-model calculations (histograms).

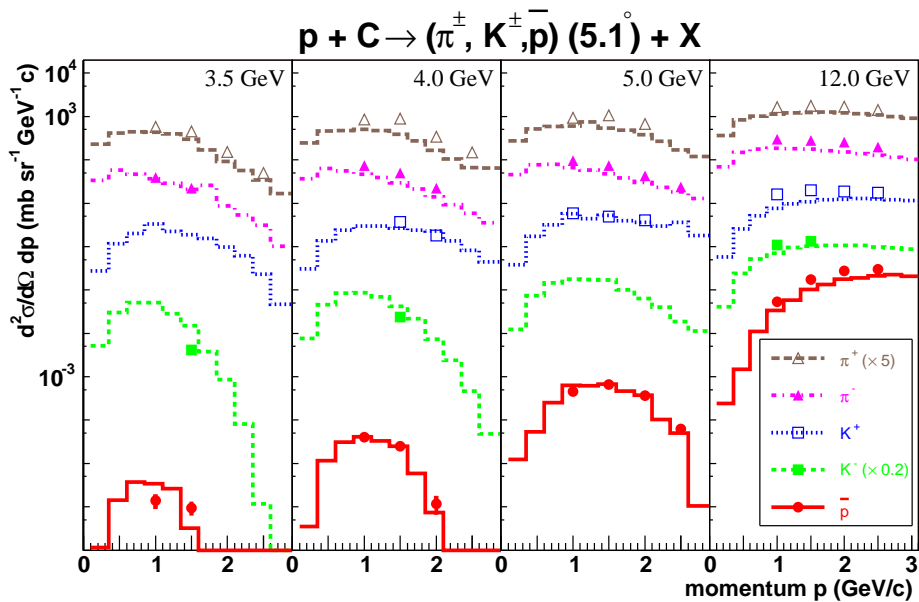


Figure 2. Momentum spectra of π^\pm , K^\pm and \bar{p} [18] (symbols) compared to ROC-model calculations (histograms). Experimental and calculated results for π^+ and K^- mesons are multiplied by the factors indicated in the legend.

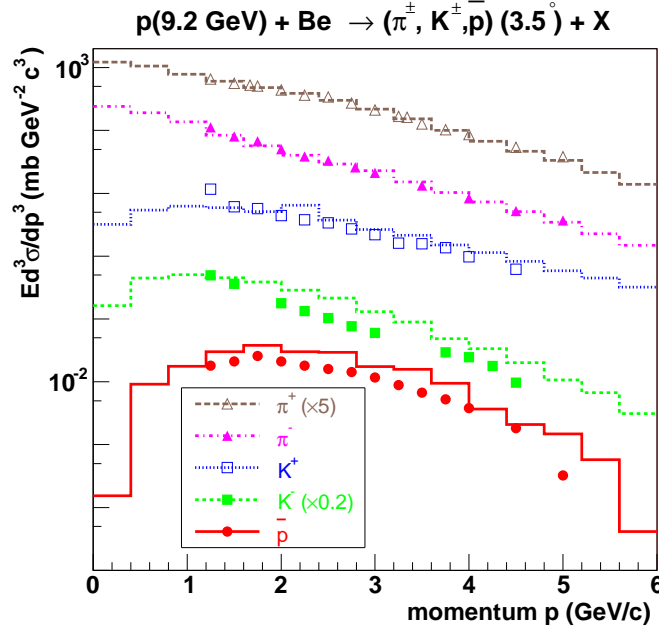


Figure 3. Momentum spectra of π^\pm , K^\pm and \bar{p} [70] (symbols) compared to ROC-model calculations (histograms). Experimental and calculated results for π^+ and K^- mesons are multiplied by the factors indicated in the legend.

compared to the KEK data [18]. The overall agreement is quite satisfactory in view of the large region of projectile energies and the variety of ejectile species calculated with one fixed parameter set. Particle yields are influenced by the suppression factor $\lambda_s = 0.15$, equation (12), of strange quarks and by the algorithm for creating the final hadrons from the quarks produced in the first stage of the interaction process. Hadrons are built up in each FB independently according to the rules of quark statistics [64] by randomly selecting sequences of q 's and \bar{q} 's. A $q\bar{q}$ gives a meson, while baryons or antibaryons are formed from qqq or $\bar{q}\bar{q}\bar{q}$. From a given sequence of quarks the different hadrons are formed according to the tables of the particle data group [65]. There is no parameter which directly determines the ratio between meson and baryon production as e.g. in the PYTHIA-LUND model [66, 67, 68, 69]. Only an indirect influence via the temperature and the volume parameter is possible, which change the relative weights of the FBs in dependence on their invariant mass and final particle multiplicity, respectively.

It is therefore quite remarkable that the general trend of the data is well reproduced by using the parameters determined in [39] from the consideration of hadronic interactions. The moderate increase with energy of the cross sections for the light mesons, the steep increase of that for the antiprotons as well as the shift of the maximum in the \bar{p} spectra towards higher momenta is well reproduced by the calculations.

At the highest energies the ROC calculations obviously tend to underestimate the data. Therefore, we compare in figure 3 as a kind of cross-check a similar data set

Table 1. ROC results for the relative contributions to the total \bar{p} cross sections at selected energies in % from terms containing various numbers $a = 1 \dots 6$ of participants as well as for the total cross sections $\sigma_{\bar{p}}$ and the cross sections $\sigma_{\bar{p}}^{\text{nf}}$ with no freezing of kinetic degrees of freedom (see text).

Energy(GeV)	1	2	3	4	5	6	$\sigma_{\bar{p}}(\text{mb})$	$\sigma_{\bar{p}}^{\text{nf}}(\text{mb})$
2.8	0.0	0.9	51.3	37.5	9.8	0.4	$7.8 \cdot 10^{-10}$	$6.3 \cdot 10^{-11}$
3.5	0.05	20.9	56.6	19.3	2.9	0.2	$1.5 \cdot 10^{-6}$	$7.9 \cdot 10^{-7}$
5.0	10.9	30.5	43.1	13.2	2.0	0.3	$2.9 \cdot 10^{-4}$	$4.3 \cdot 10^{-4}$
12.0	63.3	21.7	11.9	2.6	0.4	0.05	0.10	0.13

from [70] with ROC-model calculations. Here, the spectra are measured at a similar angle but in a much wider momentum region compared to the KEK data. In this case the tendency of the ROC results goes in the opposite direction and overestimates the cross-sections for the heavier ejectiles K^\pm and \bar{p} .

The calculated cross sections are sensitive to the assumed temperature of the residual nucleus (see figure 5). It should be stressed that the temperature derived from the fragment spectra yields also a reasonable reproduction of the \bar{p} cross sections. This point is of special importance since it demonstrates that the link between the realms of fragmentation and of hadron production made by the ROC approach is obviously correct.

The authors [18] interpret their \bar{p} data by using the “first-chance NN collision model” from [35] where the internal nucleon momenta were extracted from backward proton production [55] as a superposition of two Gaussian distributions. In this way the momentum spectra and the incident-energy dependence could be successfully reproduced by adapting one normalisation parameter. For the similar case of subthreshold K^+ production it has been, however, argued [71] that the contribution from the high-momentum component should be negligible.

In the ROC model the “first-chance NN collision” corresponds to the term in (1) describing the interaction of the projectile with a single target nucleon. In table 1 the relative contributions of the terms with a given number of participants to the total \bar{p} production cross section are summarised. It can be seen that the interaction with a single nucleon yields the main contribution only at the highest energy. The lower the energy the more contribute the terms with several target nucleons. At the lowest energy, 2.8 GeV, considered here the main contributions to \bar{p} production arise from interactions with three and four target nucleons, while quasi-free collisions are negligible. At the highest energy, 12 GeV, there are still considerable contributions from proton-cluster reactions, although quasi-free collisions became the dominating process. Thus, the interpretation of the data by the ROC model is quite contradictory to the assumptions of a “first-chance NN collision model”. From the viewpoint of the ROC model the key quantity for understanding subthreshold particle production is the number of participating nucleons. A direct experimental determination of this number for subthreshold \bar{p} production is highly desirable as discussed in [42] for the case of K^- production.

A certain similarity can be, however, found between the ROC approach and the multi-nucleon mechanism of [27], where “the incoming proton and the interacting nucleons in the target act as sources of pions that merge to produce a nucleon-antiproton pair”. In this approach the number of participating nucleons obviously

plays a similar role as in the ROC model.

Another interesting aspect of subthreshold particle production is the observation that the formation of light nuclei in the final channel alongside the produced particle(s) has to be taken into account for achieving a good reproduction of the measured cross sections. The formation of light nuclei leads to the freezing of relative kinetic energy of the nucleons, which is then available for particle production. We are speaking here about light fragments emerging from clusters, not about the decay of the residual nucleus. This effect has been discussed in [46] for pion, in [47] for photon, in [50] for K^+ production in nucleus-nucleus reactions on the basis of the cooperative model, and in [42], within the ROC model, for subthreshold K^- production in proton-nucleus interactions. In order to demonstrate the importance of this effect for subthreshold \bar{p} production we have in table 1 in addition to the “normal” ROC results $\sigma_{\bar{p}}$ also the cross sections $\sigma_{\bar{p}}^{\text{nf}}$ with no freezing listed. At the lowest energy considered the difference amounts to about one order of magnitude. This is relatively small compared to the three orders of magnitude reported by [46] for the reaction $^{12}\text{C}(85\text{MeV}/A) + ^{12}\text{C} \rightarrow \pi^+ + X$. The energy of 2.8 GeV is still far above the total production threshold of about 2.2 GeV for the coherent production at the whole target nucleus. Contrary to the energy considered in [46] also the number of competing channels is still rather high. This diminishes the influence of the neglected channels. The slight increase of $\sigma_{\bar{p}}^{\text{nf}}$ compared to $\sigma_{\bar{p}}$ at the higher energies is due to the smoother energy dependence of the relative probability $dW(s; \alpha_{az})$ of the considered channel and the smaller denominator in equation (1) as a result of neglecting a large number of final channels.

In [23, 24, 25, 28] calculations have been carried out in the framework of transport theory, where questions concerning baryon self-energies, elementary \bar{p} production amplitudes, \bar{p} potentials and \bar{p} re-absorption are of importance for the reproduction of the experimental data. In the ROC model there is no equivalent of these intra-nuclear properties implemented so far. Nuclear properties enter the ROC calculations only via the scaling (16) of the temperature and the volume of the FBs and via the excitation of the target residue caused by secondary participant-spectator interactions. Nevertheless, the spectra of all particle species are comparably well reproduced. This result should be further explored by considering heavier target nuclei, where the problem of secondary interactions becomes more important. On the other hand, the experimental investigation of \bar{p} production on the lightest nuclei as ^3He and ^4He is of special interest, since the model predicts in the energy range between 3 and 5 GeV just the 3- and 4-nucleon groups as the main source of \bar{p} production. Secondary interactions of the produced particles and the influence of the excitation of the target residue are practically absent in this case. This makes the interpretation of such data more clear than in the case of heavier target nuclei.

4. Antiproton cross section at COSY energies

Figure 4 shows a ROC-model estimate of the antiproton spectrum for a bombarding energy of 2.8 GeV averaged over a polar angle $\Theta < 10^\circ$. In order to emphasise the experimental difficulties of a measurement at such a deep subthreshold energy, the spectra of the other negative stable particles are depicted, too. In the region of the maximum in the spectra around 500 MeV/c about ten orders of magnitude more π^- mesons than antiprotons must be expected what makes a possible measurement in addition to the small \bar{p} cross section a difficult task.

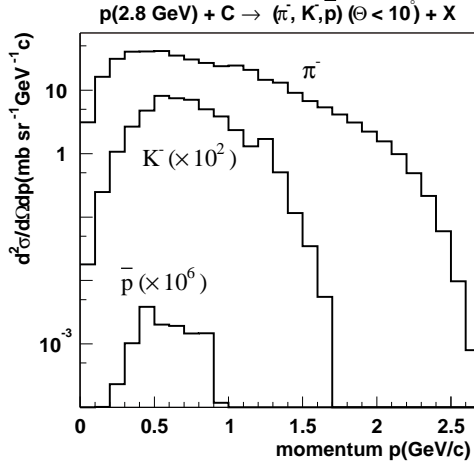


Figure 4. Momentum spectra of negatively charged hadrons calculated with the ROC model (histograms).

In figure 5 the energy dependence of the total production cross section for \bar{p} in $p + {}^{12}\text{C}$ interactions is plotted. In the energy region considered the cross section changes by more than seven orders of magnitude. The importance of the temperature of the residual nucleus at low energies is demonstrated by a calculation with the temperature arbitrarily decreased by a factor of two. This increases the cross section by about half an order of magnitude at the lowest energy. With increasing energy the influence of this parameter diminishes and becomes negligible above 10 GeV projectile energy. The Fermi motion is of similar importance for subthreshold \bar{p} production. A decrease of p_F , equation (4), by about 30% makes the \bar{p} cross section by nearly one order of magnitude smaller. Again the influence becomes negligible at high energies. These results underline once more how important it is to use a model which allows the verification of these aspects by independent measurements as has been done in this paper. It should be stressed that the selected parameter range does not reflect the uncertainty of the considered parameters which can be rather precise determined from the fragmentation data [62] (see figure 1). Instead, it is the aim to demonstrate the sensitivity of the results to the inclusion of the nuclear residue into the considerations. All results in the subthreshold region from approaches neglecting the excitation of the nuclear residue should be, therefore, taken with caution.

But also the present prediction contains of course considerable uncertainties. From our experience with existing experimental data, in particular those shown in figures 2 and 3, we know that deviations between data and calculations are usually less than a factor of two. Since any drastic change of the model feasibility is not seen if the energy decreases from 3.5 GeV to 2.8 GeV we may expect the same level of uncertainty at this lowest energy. Certainly, for the present case of a prediction rather far below the region where experimental data are available it cannot be excluded that some processes or factors not included in the ROC approach may increase their significance with the energy reduction. A possible example could be the coherent production at the whole target nucleus [72]. To be on the sure side we, therefore, assume at least the order of magnitude of the predicted cross section to be correct.

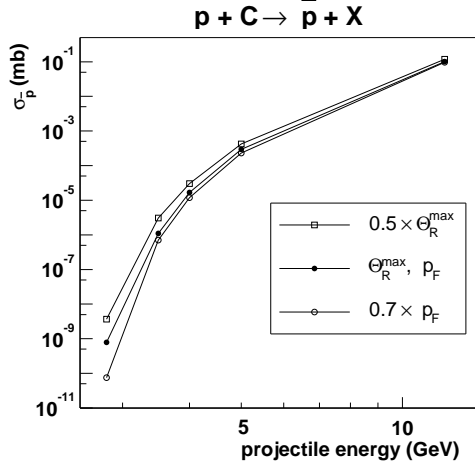


Figure 5. Cross sections of \bar{p} production as function of incident energy between 2.8 and 12.0 GeV. The \bar{p} cross sections calculated for three parameter sets (see text) are connected by straight lines.

At the ANKE spectrometer an effective detection of particles produced at angles $\lesssim 10^\circ$ in the momentum range $0.2 - 1.0$ GeV/c is possible. Assuming a luminosity of $10^{33} \text{ cm}^{-2}\text{s}^{-1}$ available with a carbon strip target and a cross section of $1 \cdot 10^{-9} \text{ mb}$ expected at 2.8 GeV one gets a counting rate at the level of five hundreds events per week of beam-time. This estimate shows the feasibility of studying \bar{p} production even at such a low subthreshold energy as considered here, if the experimental equipment allows for an efficient suppression of the negative mesons.

5. Summary

Subthreshold particle production is a collective phenomenon which is far from being completely understood. Data on subthreshold particle production can be reproduced within the ROC model by considering the interaction of the projectile with few-nucleon systems in complete analogy to the interaction with a single nucleon, also with respect to high-momentum transfer processes. It is the simultaneous consideration of the data for all particle types measured, which distinguishes the present approach from the previous attempts to interpret solely the subthreshold \bar{p} spectra from KEK. The reproduction of the data requires no strong distortion of antiprotons in nuclear matter, which might be expected due to the fact that the free $\bar{p}N$ cross section is larger than the corresponding ones for the other particle species considered. This finding needs further confirmation by measuring \bar{p} spectra at lower momenta than the region covered by the KEK data where the $\bar{p}N$ cross section increases further.

In this paper the feasibility of measuring subthreshold \bar{p} production at COSY-ANKE is demonstrated. It is argued that new insight into the mechanism of subthreshold production could be gained from an experiment nearly 3 GeV below the NN threshold, where the ROC-model calculations predict increasing contributions to the cross section from few-nucleon groups. The reliability of the predictions is verified by considering together with \bar{p} production also the results for other particles (π^\pm, K^\pm)

which could be well described in a wide energy region.

Acknowledgments

One of the authors (HM) would like to thank W Enghardt for the promotion of this study.

Appendix

The n particles of the phase-space (5) of the final state of the reaction are divided into two groups, the decay products of the residual nucleus and the particles emerging from the projectile-cluster interaction. In a first step the decay products are separated by introducing their invariant mass M_R and four-momentum P_R via the following identities:

$$1 = \int dM_R^2 \delta(P_R^2 - M_R^2) \quad (A.1)$$

$$1 = \int d^4 P_R \delta^4(P_R - \sum_{i=1}^{n_R} p_i) \quad (A.2)$$

with the definition

$$P_R = \sum_{i=1}^{n_R} p_i. \quad (A.3)$$

Inserting (A.1) . . . (A.3) into (5) the phase-space factor becomes

$$\begin{aligned} dL_n(s) = & dM_R^2 d^4 P_R \delta(P_R^2 - M_R^2) \\ & \prod_{i=1}^{n_R} d^4 p_i \delta(p_i^2 - m_i^2) \delta^4(P_R - \sum_{i=1}^{n_R} p_i) \\ & \prod_{i=1}^{n_P} d^4 p_i \delta(p_i^2 - m_i^2) \delta^4(P_P - \sum_{i=1}^{n_P} p_i). \end{aligned} \quad (A.4)$$

Taking into account that for on-shell particles the identity

$$\int d^4 p_i \delta(p_i^2 - m_i^2) = \int \frac{d^3 p_i}{2e_i} \quad (A.5)$$

is valid and considering the definition (5) of the n -particle phase-space equation (A.4) can be written as

$$dL_n(s) = dM_R^2 \frac{d^3 P_R}{2E_R} dL_{n_R}(M_R^2) dL_{n_P}(P_P^2), \quad (A.6)$$

with $n_P = n - n_R$ being the number of particles emerging from the participant interaction. The invariant mass of this participant group is given by $M_P = \sqrt{P_P^2}$ with the four-momentum $P_P = P - P_R$. The separation into two groups makes sense, because the distribution of the momentum \vec{P}_R can be derived from the internal momentum distribution $\rho(\vec{P}_R^2)$ of the target nucleus.

Inserting the matrix element (10) and the momentum distribution $\rho(\vec{P}_R^2)$ into equation (A.6) and taking the definitions (8) and (9) into account we arrive at the expression (6) for the relative probabilities of the final channels $dW(s; \alpha_{az})$.

References

- [1] Borgs W, Büscher M, Gotta D, Grzonka D and HR Koch et al 1990. *COSY Proposal #18*. Jülich
- [2] Barsov S et al. 2001 *Nucl. Instr. and Meth. A* **462** 364
- [3] Koptev V et al. 2001 *Phys. Rev. Lett.* **87** 022301. [nucl-ex/0105008](#)
- [4] Büscher M et al. 2002 *Phys. Rev. C* **65** 014603. [nucl-ex/0107011](#)
- [5] Büscher M, Koptev V, Nekipelov M et al. 2004 [nucl-ex/0401031](#)
- [6] Kirchner T et al. 1996. *COSY Proposal #21*. Jülich
- [7] Chamberlain O, Segré E, Wiegand C and Ypsilantis T 1955 *Phys. Rev.* **100** 947
- [8] Chamberlain O, Chupp W, Goldhaber G et al. 1956 *Nuovo Cimento* **3** 447
- [9] Elioff T et al. 1962 *Phys. Rev.* **128** 869
- [10] Dorfan D E et al. 1965 *Phys. Rev. Lett.* **14** 995
- [11] Baldin A et al. 1988 *JETP Lett.* **48** 137
- [12] Carroll J et al. 1989 *Phys. Rev. Lett.* **62** 1829
- [13] Shor A et al. 1989 *Phys. Rev. Lett.* **63** 2192
- [14] Schröter A et al. 1993 *Nucl. Phys. A* **553** 775c
- [15] Schröter A et al. 1994 *Z. Phys. A* **350** 101
- [16] Lepikhin Y B, Smirnitsky V A and Sheinkman V A 1987 *JETP Lett.* **46** 275
- [17] Chiba J et al. 1993 *Nucl. Phys. A* **553** 771c
- [18] Sugaya Y et al. 1998 *Nucl. Phys. A* **634** 115
- [19] Li G Q, Ko C M, Fang X S and Zheng Y M 1994 *Phys. Rev. C* **49** 1139
- [20] Batko G, Cassing W, Mosel U, Niita K and Wolf G 1991 *Phys. Lett. B* **256** 331
- [21] Huang S W, Li G, Maruyama T and Faessler A 1992 *Nucl. Phys. A* **547** 653
- [22] Cassing W, Lang A, Teis S and Weber K 1994 *Nucl. Phys. A* **545** 123c
- [23] Teis S, Cassing W, Maruyama T and Mosel U 1993 *Phys. Lett. B* **319** 47
- [24] Teis S, Cassing W, Maruyama T and Mosel U 1994 *Phys. Rev. C* **50** 388
- [25] Cassing W, Lykasov G and Teis S 1994 *Z. Phys. A* **348** 247
- [26] Batko G, Faessler A, Huang S, Lehmann E and Rajeev K 1994 *J. Phys. G* **20** 461
- [27] Hernández E, Oset E and Weise W 1995 *Z. Phys. A* **351** 99
- [28] Sibirtsev A, Cassing W, Lykasov G I and Rzjanin M V 1998 *Nucl. Phys. A* **632** 131
- [29] Koch P and Dover C B 1989 *Phys. Rev. C* **40** 145
- [30] Ko C M and Ge X 1988 *Phys. Lett. B* **205** 195
- [31] Ko C M and Xia L H 1989 *Phys. Rev. C* **40** R1118
- [32] D'yachenko A T 2000 *J. Phys. G* **26** 861
- [33] Danielewicz P 1990 *Phys. Rev. C* **42** 1564
- [34] Müller H and Sistemich K 1992 *Z. Phys. A* **344** 197
- [35] Shor A, Perez-Mendez V and Ganezer K 1990 *Nucl. Phys. A* **514** 717
- [36] Kahana S H, Pang Y, Schlagel T and Dover C B 1993 *Phys. Rev. C* **47** R1356
- [37] Abbott T et al. 1993 *Phys. Rev. C* **47** R1351
- [38] Müller H 1995 *Z. Phys. A* **353** 103
- [39] Müller H 2001 *Eur. Phys. J. C* **18** 563. <http://arXiv.org/hep-ph/0011350>
- [40] Müller H 1991 *Z. Phys. A* **339** 409
- [41] Müller H 1995 *Z. Phys. A* **353** 237
- [42] Müller H 1996 *Z. Phys. A* **355** 223
- [43] Knoll J 1979 *Phys. Rev. C* **20** 773
- [44] Knoll J 1980 *Nucl. Phys. A* **343** 511
- [45] Bohrmann S and Knoll J 1981 *Nucl. Phys. A* **356** 498
- [46] Shyam R and Knoll J 1984 *Nucl. Phys. A* **426** 606
- [47] Shyam R and Knoll J 1986 *Nucl. Phys. A* **448** 322
- [48] Knoll J and Shyam R 1988 *Nucl. Phys. A* **483** 711
- [49] Ghosh B and Shyam R 1990 *Phys. Lett. B* **234** 248
- [50] Ghosh B 1992 *Phys. Rev. C* **45** R518
- [51] Shmakov S, Uzhinskii V and Zadorozhny A 1988 *Comp. Phys. Communications* **54** 125
- [52] Glauber R J and Mathiae J 1970 *Nucl. Phys. B* **21** 135
- [53] Elton L R 1961 *Nuclear sizes/L. R. B. Elton* (London : Oxford Univ. Pr.)
- [54] Goldhaber A S 1974 *Phys. Lett. B* **53** 306
- [55] Geaga J V et al. 1980 *Phys. Rev. Lett.* **45** 1993
- [56] Ciofi degli Atti C and Simula S 1996 *Phys. Rev. C* **53** 1689
- [57] Benhar O, Fabrocini A and Fantoni S 1989 *Nucl. Phys. A* **505** 267
- [58] Sick I, Fantoni S, Fabrocini A and Benhar O 1994 *Phys. Lett. B* **323** 267

- [59] Sibirtsev A, Cassing W and Mosel U 1997 *Z. Phys. A* **358** 357
- [60] Byckling E and Kajantie K 1973 *Particle Kinematics* (John Wiley and Sons, London, New York, Sydney, Toronto)
- [61] Bondorf J *et al.* 1985 *Nucl. Phys. A* **443** 321
- [62] Westfall G *et al.* 1978 *Phys. Rev. C* **17** 1368
- [63] Bondorf J, Botvina A, Iljinov A, Mishustin I and Sneppen K 1995 *Phys. Rep.* **257** 133
- [64] Anisovich V V and Shekhter V M 1973 *Nucl. Phys. B* **55** 455
- [65] Caso C *et al.* 1998 *Eur. Phys. J. C* **3** 1
- [66] Andersson B, Gustafson G, Ingelman G and Sjöstrand T 1983 *Phys. Rep.* **97** 31
- [67] Andersson B, Gustafson G and Nilsson-Almqvist B 1987 *Nucl. Phys. B* **281** 289
- [68] Sjöstrand T and van Zijl M 1987 *Phys. Rev. D* **36** 2019
- [69] Sjöstrand T 1994 *Comput. Phys. Commun.* **82** 74
- [70] Vorontsov I A, Safronov G A, Sibirtsev A A, Smirnov G N and Trebukhovsky Y V 1988 ITEP-11-1988
- [71] Sibirtsev A 1995 *Phys. Lett.* **359** 29
- [72] Lopez-Alvaredo B *et al.* 1996 *Nucl. Phys. A* **611** 568